

# Arabidopsis Copper Transport Protein COPT2 Participates in the Cross Talk between Iron Deficiency Responses and Low-Phosphate Signaling<sup>1[C][W]</sup>

Ana Perea-García<sup>2</sup>, Antoni Garcia-Molina<sup>2,3</sup>, Nuria Andrés-Colás, Francisco Vera-Sirera, Miguel A. Pérez-Amador, Sergi Puig<sup>4</sup>, and Lola Peñarrubia\*

Departament de Bioquímica i Biologia Molecular, Universitat de València, ES-46100 Burjassot, Valencia, Spain (A.P.-G., A.G.-M., N.A.-C., S.P., L.P.); and Instituto de Biología Molecular y Celular de Plantas, Consejo Superior de Investigaciones Científicas-Universidad Politécnica de Valencia, ES-46022 Valencia, Spain (F.V.-S., M.A.P.-A.)

Copper and iron are essential micronutrients for most living organisms because they participate as cofactors in biological processes, including respiration, photosynthesis, and oxidative stress protection. In many eukaryotic organisms, including yeast (*Saccharomyces cerevisiae*) and mammals, copper and iron homeostases are highly interconnected; yet, such interdependence is not well established in higher plants. Here, we propose that COPT2, a high-affinity copper transport protein, functions under copper and iron deficiencies in *Arabidopsis thaliana*. COPT2 is a plasma membrane protein that functions in copper acquisition and distribution. Characterization of the COPT2 expression pattern indicates a synergic response to copper and iron limitation in roots. We characterized a knockout of COPT2, *copt2-1*, that leads to increased resistance to simultaneous copper and iron deficiencies, measured as reduced leaf chlorosis and improved maintenance of the photosynthetic apparatus. We propose that COPT2 could play a dual role under iron deficiency. First, COPT2 participates in the attenuation of copper deficiency responses driven by iron limitation, possibly to minimize further iron consumption. Second, global expression analyses of *copt2-1* versus wild-type *Arabidopsis* plants indicate that low-phosphate responses increase in the mutant. These results open up new biotechnological approaches to fight iron deficiency in crops.

Copper (Cu) and iron (Fe) act as a double-edged sword in living beings, since they are essential redox-active micronutrients but are cytotoxic when in excess. Since both metals participate as catalytic cofactors in multiple metabolic pathways, their homeostasis needs to be strictly controlled. Plants are the basis of trophic chains, and their nutritional deficiencies are often

transferred to consumers. The essentiality of Cu and Fe in plants is evidenced by the symptoms that their deficiencies provoke, which affect the yield and nutritional value of crops (Märschner, 2002; Puig et al., 2007). In biological terms, use of Fe preceded Cu due to the high bioavailability of Fe as Fe<sup>2+</sup> under anoxic conditions. However, the appearance of oxygen in the atmosphere caused not only reduced Fe bioavailability but also concomitantly increased the bioavailability and use of Cu by biological systems (Crichton and Pierre, 2001). In parallel with the incorporation of Cu into multiple processes requiring higher redox potentials, which temporally coincided with the commencement of pluricellularity, new strategies to solubilize and acquire Fe<sup>3+</sup> were developed. In some cases, enzymes that catalyze the same biochemical reaction are coordinately regulated to allow the alternative use of either Cu- or Fe-containing proteins, depending on metal bioavailability. One main example in *Arabidopsis thaliana* plants is the use of copper/zinc superoxide dismutase (Cu/ZnSOD) versus iron superoxide dismutase (FeSOD), which both play roles in reactive oxygen species detoxification (Abdel-Ghany et al., 2005; Yamasaki et al., 2007; Burkhead et al., 2009; Waters et al., 2012).

In *Arabidopsis*, deciphering responses to Cu deficiency is now starting (Pilon et al., 2009; Peñarrubia et al., 2010). A family of high-affinity Cu transport proteins, denoted COPTs in plants (CTR in yeast [*Saccharomyces*

<sup>1</sup> This work was supported by the Spanish Ministry of Economy and Competitiveness (grant nos. BIO2011-24848 and CSD2007-00057 to L.P. and predoctoral Formación Personal Investigador fellowships to A.P.-G and A.G.-M.) and by the European Regional Developmental Fund of the European Union.

<sup>2</sup> These authors contributed equally to the article.

<sup>3</sup> Present address: Molecular Plant Genetics Department, Max Planck Institute for Plant Breeding, Carl-von-Linne-Weg 10, D-50829 Cologne, Germany.

<sup>4</sup> Present address: Departamento de Biotecnología, Instituto de Agroquímica y Tecnología de Alimentos-Consejo Superior de Investigaciones Científicas, Avenida Agustín Escardino 7, E-46980 Paterna (Valencia) Spain.

\* Corresponding author; e-mail penarrub@uv.es.

The author responsible for distribution of materials integral to the findings presented in this article in accordance with the policy described in the Instructions for Authors ([www.plantphysiol.org](http://www.plantphysiol.org)) is: Lola Peñarrubia (penarrub@uv.es).

[C] Some figures in this article are displayed in color online but in black and white in the print edition.

[W] The online version of this article contains Web-only data.

[www.plantphysiol.org/cgi/doi/10.1104/pp.112.212407](http://www.plantphysiol.org/cgi/doi/10.1104/pp.112.212407)

*cerevisiae*] and human), participates in Cu transport toward the cytosol. COPT1 is a plasma membrane-located member of this family that plays a key role in Cu uptake, root growth, and pollen development (Kampfenkel et al., 1995; Sancenón et al., 2004). Recent studies have shown that deregulated Cu transport in *COPT1*-overexpressing plants affects development under continuous environmental conditions (Andrés-Colás et al., 2010). On the other hand, Cu activates calcium- and potassium-permeable plasma membrane transporters in *COPT1*-overexpressing plants under 10  $\mu\text{M}$  Cu conditions, which might be caused by the generation of a cytosolic hydroxyl radical (Rodrigo-Moreno et al., 2013). In the COPT family, *COPT1* and *COPT2* mRNA levels are down-regulated by Cu, and their expression completely rescues the respiratory defect of yeast *ctr1 $\Delta$ ctr3 $\Delta$*  mutants, which are defective in high-affinity Cu uptake (Sancenón et al., 2003). The Arabidopsis genome encodes a 17-member zinc finger plant-specific transcription factor family named SPL (for SQUAMOSA-promoter binding-like proteins; Birkenbihl et al., 2005). SPL7 has been shown to be essential for the transcriptional activation observed in response to Cu deficiency in vivo through its binding to GTAC motifs within the promoter of Cu-responsive genes, including those encoding COPT1, COPT2, and the FeSOD FSD1 (Yamasaki et al., 2009; Bernal et al., 2012).

Despite its abundance in soils, Fe bioavailability is very limited, which often provokes Fe deficiency symptoms (i.e. chlorosis) and lowers crop yields. The primary response of Arabidopsis plants to Fe deficiency is controlled through coordinated transcriptional activation, including the increased expression of metal reductases and transporters, such as *Ferric reduction oxidase2* (*FRO2*) and *Iron-regulated transporter1* (*IRT1*), respectively, to improve metal bioavailability and acquisition. The Arabidopsis basic helix-loop-helix (bHLH) transcription factor bHLH29/FRU, also known as FIT (for Fe deficiency-induced transcription factor), controls some of the root responses upon Fe limitation at different levels (for review, see Guerinot, 2000; Hindt and Guerinot, 2012; Ivanov et al., 2012).

Fe availability has been shown to play a crucial role in the root architecture changes induced by phosphate (Pi) deficiency in Arabidopsis (Ward et al., 2008). Thus, whereas primary root elongation is greatly inhibited by Pi starvation, root growth is restored under reduced Fe without increasing Pi availability (Ward et al., 2008). Moreover, Pi-starved Arabidopsis plants show elevated Fe accumulation in both shoots and roots (Misson et al., 2005; Ward et al., 2008). Phosphorus is not only an essential macronutrient but also a key component of, among others, membrane phospholipids and is crucial for processes such as signaling cascades (Raghothama, 1999; Chiou and Lin, 2011). It has been suggested that Pi may be sensed indirectly via complex and antagonistic interactions between Pi and Fe availabilities, which still remain to be elucidated (Abel, 2011).

Given their sessile nature, plants are organisms that probably explore the widest variety of responses to environmental nutrient availabilities, and they have developed multiple regulatory mechanisms to respond to metal and nutrient deficiencies. In addition to the aforementioned substitution of specific metalloproteins, improved metal bioavailability and acquisition, including the increased expression of metalloreductases and high-affinity transporters, are among the main strategies to help face metal deficiencies (Jeong and Guerinot, 2009; Palmer and Guerinot, 2009; Puig and Peñarrubia, 2009). Nutrient status information has to be communicated between organs to optimize essential inorganic nutrient allocation, especially in plants growing under suboptimal conditions. Root architecture is differentially modified during nutrient deficiencies. Whereas root elongation is considered an adequate modification under metal deficiencies, possibly to seek metals in underground soil layers, the inhibition of primary root growth and the development of secondary and higher order roots under Pi starvation maximize the interception of the nutrient in top soil layers (Liao et al., 2001). These processes exemplify not only the extensive cross talk between different metals and other nutrient homeostasis networks but also the delicate balance that plant cells have to strike according to the variable nutritional status in the environment.

In this study, we analyzed the function of the high-affinity Cu transport protein COPT2, whose expression in Arabidopsis is up-regulated in roots by both Cu and Fe deficiencies (Sancenón et al., 2003; Colangelo and Guerinot, 2004; Waters et al., 2012), whereas Pi starvation diminishes its expression (Thibaud et al., 2010). The phenotypes and gene expression changes displayed by a *copt2-1* line reveal a role for COPT2 in the cross talk among Cu, Fe, and Pi deficiency responses in Arabidopsis.

## RESULTS

### The High-Affinity Cu Transport Protein COPT2 Localizes to the Plasma Membrane of Arabidopsis Cells

The *COPT2* gene (*At3g46900*) from Arabidopsis encodes a protein with a 78% identity with COPT1 (Kampfenkel et al., 1995; Sancenón et al., 2003; Supplemental Fig. S1A). The hydrophobicity pattern and the topological comparison between COPT2 and other CTR/COPT family members indicate the presence of three transmembrane domains (TMDs) with an external N terminus and a cytosolic C terminus (Supplemental Fig. S1B). Moreover, it possesses the conserved extracellular Met residue (indicated by asterisks in Supplemental Fig. S1) before TMD1, the MxxxM motif in TMD2, and the GxxxG motif in TMD3, which are essential in yeast homologs (Puig et al., 2002; Aller et al., 2004). A CxC motif is also observed in the COPT2 C-terminal domain (Supplemental Fig. S1). Given its ability to fully complement the respiratory defects of yeast

*ctr1Δctr3Δ* mutants and its regulation by environmental Cu in Arabidopsis, it has been previously suggested that both the COPT2 and COPT1 proteins could function in Cu acquisition in the plasma membrane of specific plant cells (Kampfenkel et al., 1995; Sancenón et al., 2003, 2004).

For the purpose of localizing COPT2 at the subcellular level in Arabidopsis cells, its coding sequence was fused to the GFP (*COPT2-GFP*) under the control of the constitutive *CaMV35S* promoter. As shown in Figure 1A, the construct *COPT2-GFP* complements the respiratory defect of yeast *ctr1Δctr3Δ* mutants to a similar extent as *COPT2* and *COPT1*, indicating that addition of the GFP does not interfere with the Cu transport function in yeast. Isolated Arabidopsis protoplasts transiently expressing the *PCaMV35S:COPT2:GFP* construct were analyzed for the localization of COPT2-GFP, lipophilic styryl dye FM4-64, and chlorophyll fluorescences indicated by green, cyan, and magenta, respectively (Fig. 1B). In addition to the chlorophyll autofluorescence, *COPT2-GFP*-expressing cells display a signal on the cell surface that is absent in vacuoles, the cytosol, and other discrete subcellular localizations. This signal colocalizes with the FM4-64 marker, which localizes to the cell surface at low temperatures (Fig. 1B). Furthermore, immunofluorescence labeling of stable transgenic

Arabidopsis plants expressing the *CaMV35S:COPT2-HA* construct shows a signal restricted to the peripheral side of the cytoplasm when using anti-hemagglutinin (HA) antibodies (Supplemental Fig. S2). These results strongly suggest that the COPT2 protein localizes to the plasma membrane of Arabidopsis cells.

### *COPT2* Expression Is Differentially Regulated by Cu and Fe Deficiencies

In order to study the *COPT2* spatial expression pattern, the promoter region (*PCOPT2*; covering 1,248 bp upstream from the start codon) was fused to the *uidA* (*GUS*) reporter gene. Transgenic Arabidopsis lines harboring the *PCOPT2:GUS* chimeric gene were obtained. *GUS* staining in 7-d-old Arabidopsis seedlings grown under Cu-deficient conditions indicated that *COPT2* was expressed in most tissues of the seedlings (Fig. 2A). For roots, *GUS* staining was observed in the differentiation zone but was absent from the elongation and meristematic zones (Fig. 2, B and C). Moreover, *COPT2* expression in roots included the lateral roots and root hairs, displaying expression mostly in the epidermis (Fig. 2D). In cotyledons, the highest expression was observed in vascular bundles and

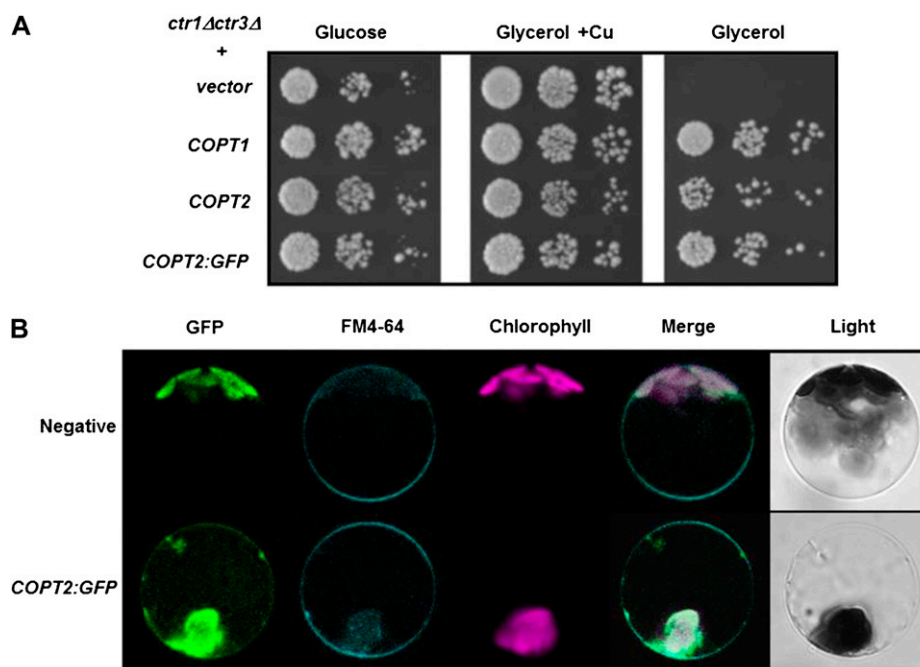


**Figure 1.** *COPT2:GFP* functionality in yeast, and subcellular localization in Arabidopsis protoplasts. A, Yeast *ctr1Δctr3Δ* cells were transformed with p426GPD, *COPT1*, *COPT2*, and *COPT2:GFP* and were spotted on synthetic complete-ura medium (Glucose) or yeast extract peptone glycerol (Glycerol) supplemented with 100  $\mu\text{M}$   $\text{CuSO}_4$  (Glycerol + Cu). Each spot represents a 1:10 cell culture density dilution, decreasing from left to right. B, Arabidopsis protoplasts were isolated from 30-d-old leaves and were transiently transformed with the *PCaMV35S:COPT2:GFP* construct, incubated with FM4-64 for 15 min at 4°C, before being analyzed by confocal microscopy at 16 h post transformation. Nontransformed protoplasts were used as a negative control. Green, cyan, and magenta fluorescences are indicative of the localization of the GFP protein, the FM4-64 marker, and chlorophyll, respectively. Representative protoplasts are shown on the same scale, including their merged and light fields.

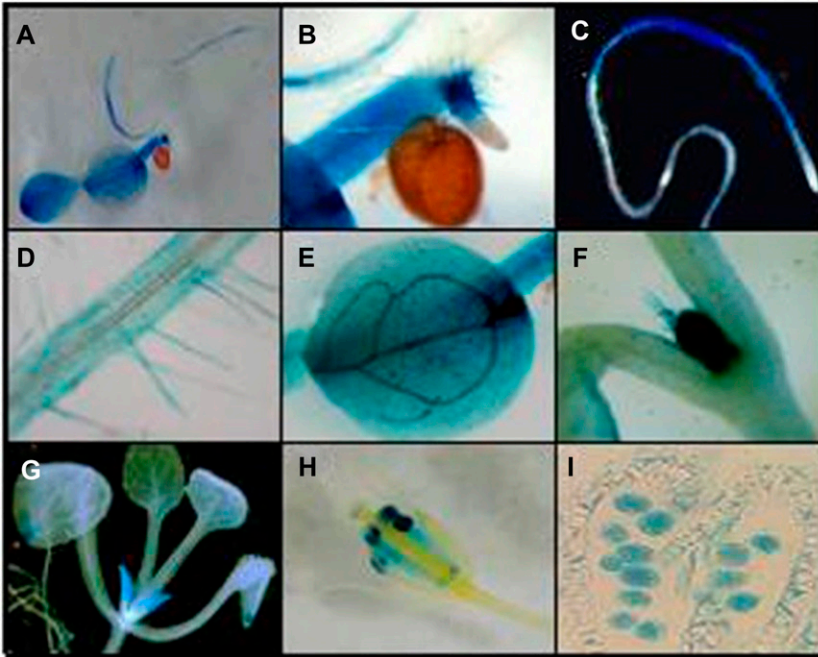


**Figure 2.** *COPT2* expression pattern in Arabidopsis *PCOPT2:GUS* transgenic plants under Cu deficiency. Shown are GUS staining in a representative 7-d-old seedling (A), detail of a secondary root tip (B), general view of the main root (C), detail of root hairs (D), cotyledon (E), shoot meristem and trichomes (F), aerial part from a 3-week-old seedling (G), flower (H), and a longitudinal section of an anther with pollen grains (I).

hydathodes (Fig. 2E). Histological analyses of seedlings and adult plants showed *COPT2* promoter-driven GUS expression in the apical meristem and trichomes (Fig. 2F) and in young leaves (Fig. 2G). During the development of reproductive organs, the GUS staining in anthers (Fig. 2H) indicates that *COPT2* is highly expressed in pollen (Fig. 2I). Three other independent *PCOPT2:GUS* lines were analyzed and showed the same *COPT2* tissue pattern expression (data not shown). Schematics of the *COPT2*, as compared with the *COPT1*, expression patterns, along with other characteristics of both permeases, are shown in Supplemental Figure S3.

The analysis of the regulatory elements in the *PCOPT2* region indicates the presence of four GTAC motifs, which are probably involved in its regulation by Cu (Supplemental Fig. S4; Yamasaki et al., 2009). Interestingly, *COPT2* is the *COPT* family member whose expression was most highly regulated by Cu deficiency (Sancenón et al., 2003; Yamasaki et al., 2009; del Pozo et al., 2010). In addition, a putative E-box consensus, which may be involved in the interaction with bHLH-type transcription factors such as the Fe-responsive FIT protein (Hartmann et al., 2005), was present in its promoter (Supplemental Fig. S4). Accordingly, *COPT2* expression has been shown to respond to Fe deficiency in a partially FIT-dependent manner (Colangelo and Guerinot, 2004). To ascertain *COPT2* expression under separate Fe and Cu deficiencies, or when both deficiencies are applied simultaneously, wild-type seedlings were grown in the four following media combinations: first, Fe- and Cu-sufficient medium (+Fe+Cu; one-half-strength Murashige and Skoog medium [1/2 MS] supplemented with  $10 \mu\text{M}$   $\text{CuSO}_4$ ); second, Fe-sufficient and Cu-deficient medium (+Fe-Cu; 1/2 MS without  $\text{CuSO}_4$ ); third, Fe-deficient and Cu-sufficient medium

(-Fe+Cu; 1/2 MS without Fe and supplemented with  $10 \mu\text{M}$   $\text{CuSO}_4$  and  $300 \mu\text{M}$  ferrozine, a specific  $\text{Fe}^{2+}$  chelator); and fourth, Fe- and Cu-deficient medium (-Fe-Cu; 1/2 MS without Cu and Fe and supplemented with  $300 \mu\text{M}$  ferrozine). The Cu concentration used in this experiment was  $10 \mu\text{M}$ , which was high enough to guarantee a sufficient Cu supply while being far from the deficiency and excess responses (Andrés-Colás et al., 2010). *COPT2* expression was induced by Cu deficiency (35.6-fold), by Fe deficiency (4.3-fold), and its expression was further increased under simultaneous Fe and Cu deprivation (52.3-fold; Fig. 3A; Supplemental Table S1). *COPT2* expression remained mostly under the control of the *SPL7* transcription factor, since the *spl7* mutant displayed a significant drop at the mRNA levels (Fig. 3A; Yamasaki et al., 2009; Bernal et al., 2012). However, *COPT2* was still expressed at low basal levels under all the conditions tested in the *spl7* mutant as compared with a *copt2* null mutant (*copt2-1* line [see below]; Fig. 3A), indicating that this basal expression level was *SPL7* independent. Furthermore, the *COPT2* tissue pattern shows that under Cu deficiency (+Fe-Cu), it was highly expressed in roots and that its expression increased under both metal deficiencies (-Fe-Cu; Fig. 3B). In order to further define where *COPT2* expression started, root photographs under 1 h at  $37^\circ\text{C}$  for GUS staining were obtained, showing cell patches of differentiated root cells (Fig. 3B). Interestingly, high ( $1 \mu\text{M}$ ) Cu levels (+Fe+Cu) completely abolished *COPT2* expression in roots, but a low expression level, which requires overnight GUS staining, remained restricted to cotyledons under Fe deficiency (-Fe+Cu; Fig. 3B). The expression in roots requires Cu deficiency conditions, and it was not observed under Fe deficiency when the Cu levels in the

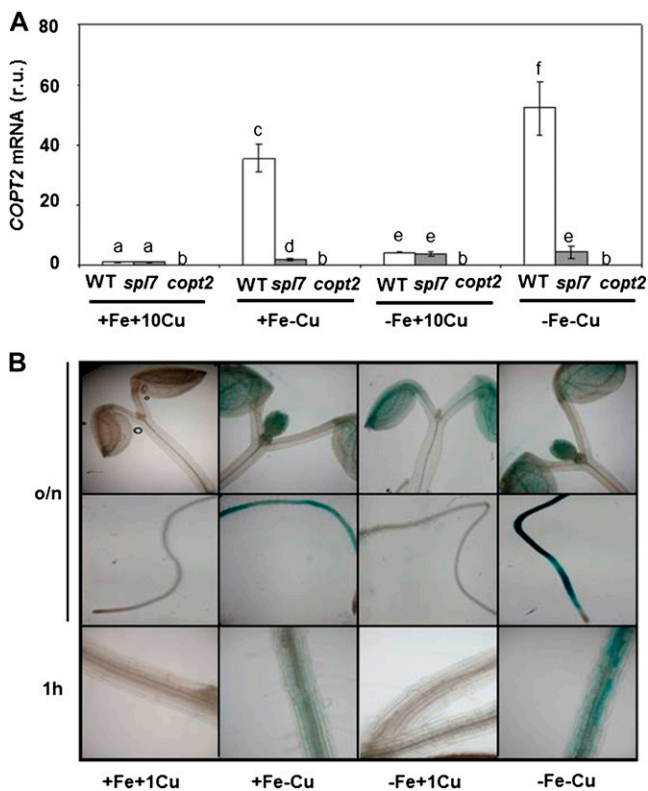


**Figure 3.** *COPT2* expression under Cu and Fe deficiencies. A, *COPT2* expression analysis by qPCR in wild-type (WT; white bars), *spl7* (gray bars), and *copt2-1* (*copt2*; dark gray bars) seedlings. Total RNA from 7-d-old seedlings grown under the control (+Fe+Cu; supplemented with 10  $\mu\text{M}$   $\text{CuSO}_4$ ), Cu deficiency (+Fe–Cu), Fe deficiency (–Fe+Cu; supplemented with 10  $\mu\text{M}$   $\text{CuSO}_4$ ), or Fe and Cu deficiency (–Fe–Cu) conditions was isolated and retrotranscribed to complementary DNA. *UBQ10* gene expression was used as a loading control. Values are means  $\pm$  SD of three biological replicates. r.u., Relative units. Different letters above the bars represent significant differences among all the means ( $P < 0.05$ ). B, GUS staining in 7-d-old seedlings from the *PCOPT2:GUS* transgenic lines grown under control (+Fe+Cu; supplemented with 1  $\mu\text{M}$   $\text{CuSO}_4$ ), Cu deficiency (+Fe–Cu), Fe deficiency (–Fe+Cu; supplemented with 1  $\mu\text{M}$   $\text{CuSO}_4$ ), or Fe and Cu deficiency (–Fe–Cu) conditions at different incubation times at 37°C (overnight [o/n] and 1 h). [See online article for color version of this figure.]

medium were higher than 0.25  $\mu\text{M}$  (Supplemental Fig. S5). However, the low expression in cotyledons was observed at higher Cu levels under overnight GUS-staining conditions (Fig. 3B; Supplemental Fig. S5). Taken together, these results not only demonstrate that *COPT2* expression is differentially regulated by low Cu and Fe conditions but suggest a cross talk between both metal deficiencies.

#### Characterization of the *copt2-1* Line under Cu and Fe Deficiency Conditions

A *copt2-1* line (Supplemental Fig. S6) that contains the transfer DNA (T-DNA) insert at –55 bp (in relation to the translation start codon), separating the four

putative Cu regulatory GTAC motifs from the *COPT2* coding sequence (Supplemental Fig. S6A), shows no *COPT2* expression in seedlings grown on different Cu availabilities (100  $\mu\text{M}$  bathocuproinedisulfonic acid disodium and 0, 1, 5, or 10  $\mu\text{M}$   $\text{CuSO}_4$ ; Supplemental Fig. S6C). Moreover under the four conditions previously stated for Cu and Fe availability, the *COPT2* expression levels in the *copt2-1* line were below those found in the *spl7* mutant (Fig. 3A). Therefore, we used the *copt2-1* mutant to study the function of this transporter in Arabidopsis.

Since *COPT2* displays different expression patterns under +Fe–Cu, –Fe+Cu, and –Fe–Cu conditions, we studied the potential *copt2-1* phenotypes under these conditions as compared with the +Fe+Cu control medium. Apparently, the mutant did not seem to differ from the wild-type controls when grown on soil or in 1/2 MS with different Cu availabilities. Furthermore, certain parameters, such as root length, seed germination, deetiolation, and hypocotyl length, showed no significant differences between the wild type and the *copt2-1* line under the different Cu statuses analyzed (data not shown). However, whereas the wild-type plants grown under simultaneous Cu and Fe deficiency conditions exhibited a light green leaf appearance, a typical symptom of mild chlorosis, the *copt2-1* seedlings displayed a slightly increased resistance to Fe deprivation by delaying symptoms, as shown by their greener leaves (Fig. 4A). In order to quantify this *copt2-1* phenotype, total chlorophylls were measured in 7-d-old wild-type and mutant seedlings grown under the four Fe/Cu conditions stated above. As Figure 4B illustrates, the *copt2-1* line showed increased chlorophylls when compared with the wild-type seedlings, especially under –Fe conditions. Despite no significant changes in fresh weight being detected under Fe deficiency (Supplemental Fig. S7A), a parameter indicative of photosynthetic apparatus integrity such as *LHCBI.1* (for light-harvesting complex B1.1) mRNA, showed a slightly higher level in the mutant than in the wild-type plants under Fe deficiency conditions (Supplemental Fig. S7B). In order to ascertain whether these defects were *COPT2* specific, we transformed the *copt2-1* line with the *COPT2* wild-type gene driven by its own promoter (*PCOPT2:COPT2:GFP*). Importantly, the *PCOPT2:COPT2:GFP* seedlings grown under both metal deficiencies revealed a partial restoration of *COPT2* expression and, accordingly, displayed an increased sensitivity to metal deficiencies, as shown by the chlorophyll content (Fig. 5). Moreover, the *LHCBI.1* and *FSD1* expression decreased when compared with the *copt2-1* line under simultaneous metal deficiency (Fig. 5C), which is in agreement with reduced plant performance in the presence of *COPT2* expression. The *copt1* mutant also displayed a similar phenotype of resistance to Fe deficiency-induced chlorosis (data not shown), which further corroborates the role of Cu in this process. To investigate whether the better resistance of the mutant to ferric chlorosis under –Fe–Cu conditions was also

displayed in adult stages, plants were grown in hydroponic cultures under +Fe+Cu (Hoagland) and -Fe-Cu (Hoagland with no added Cu and Fe) conditions. As indicated for the seedlings grown on agar plates (Figs. 4 and 5), once again the chlorosis under -Fe-Cu conditions in the aerial part was less pronounced or retarded in the *copt2-1* line than in the wild-type adult plants (Fig. 6). It is worth noting that the plastocyanin content in the leaves of the adult plants grown under -Fe-Cu conditions was higher in the *copt2-1* line than in wild-type plants (Supplemental Fig. S8). Moreover, senescence of the *copt2-1* siliques is delayed compared with the wild type (Supplemental Fig. S9A), and subsequently, the mutant produces more seeds (Supplemental Fig. S9B) with a higher germination rate (40%) than wild-type plants (5%) when grown under both metal deficiency conditions. Taken together, these results further support the better or extended maintenance of the photosynthetic apparatus in the *copt2-1* line than in the wild-type plants grown under conditions of simultaneous Fe and Cu deficiencies, which leads to improved plant growth and seed production.

In order to determine whether the total endogenous metal content in these plants was responsible for the

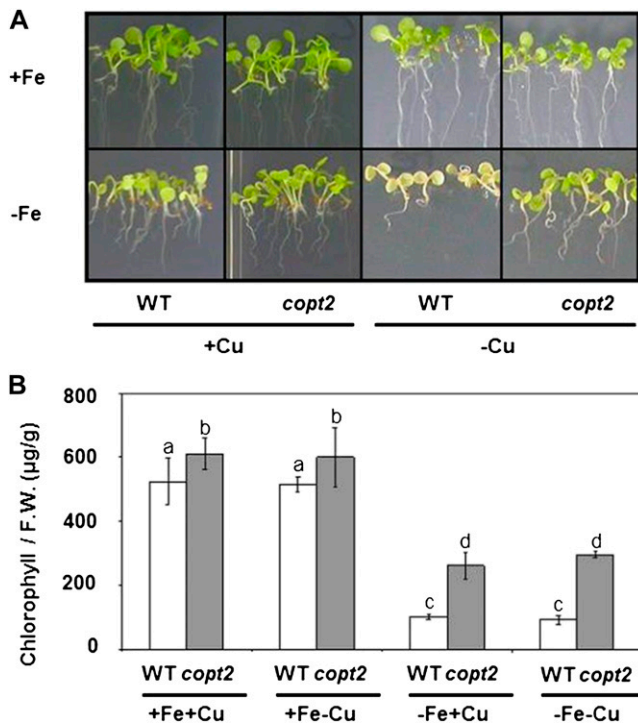


**Figure 4.** Phenotypes of the *copt2-1* seedlings grown under Cu and Fe deficiencies. A, Photographs of 7-d-old seedlings of the wild type (WT) and the *copt2-1* line grown under the same conditions described in Figure 3A. B, Chlorophyll contents of 7-d-old seedlings of both the wild type (white bars) and *copt2* (gray bars) grown under the same conditions described in Figure 3. Values are means  $\pm$  SD of at least three biological replicates. F.W., Fresh weight. Different letters above the bars represent significant differences among all the means ( $P < 0.05$ ).

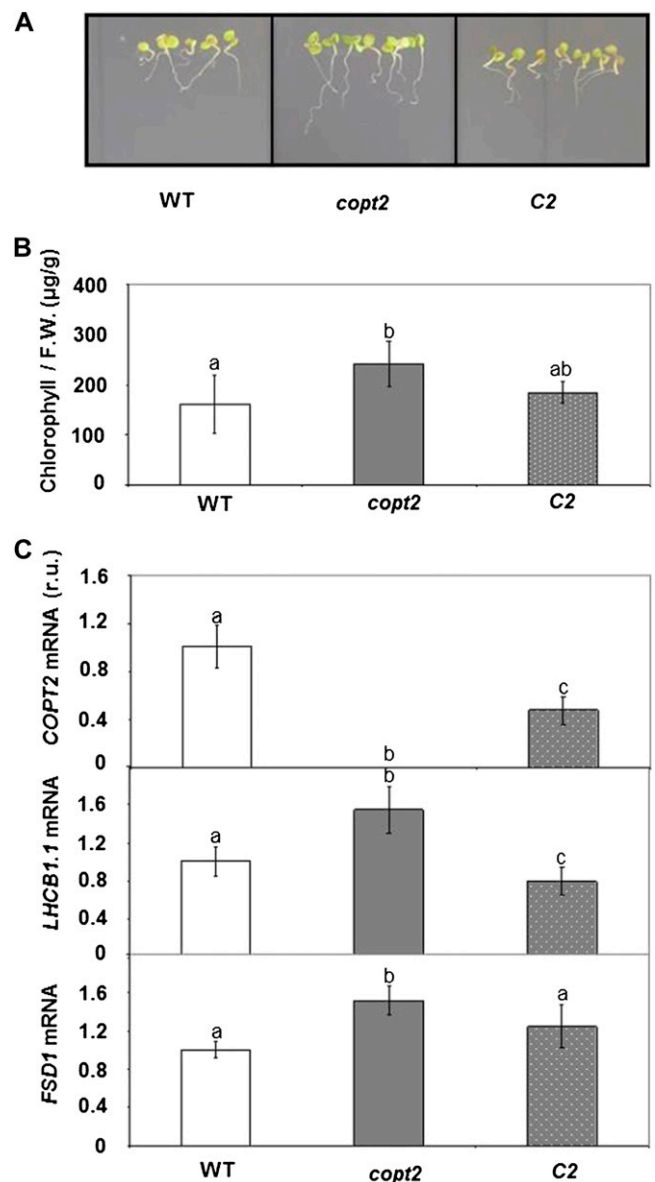


**Figure 5.** Chlorophyll contents and gene expression of complemented *copt2-1* seedlings grown under Cu and Fe deficiencies. A, Photographs of 7-d-old seedlings of the wild type (WT), *copt2-1* (*copt2*), and *PCOPT2:COPT2:GFP* (C2) grown under -Fe-Cu conditions. B, Chlorophyll contents of wild-type (white bars), *copt2* (gray bars), and C2 (dotted bars) seedlings. Values are means  $\pm$  SD of at least four biological replicates. Different letters above the bars represent significant differences among all the means ( $P < 0.01$ ). F.W., Fresh weight. C, Expression analysis of *COPT2*, *LHCb1.1*, and *FSD1* genes by qPCR in wild-type (white bars), *copt2* (gray bars), and C2 (dotted bars) seedlings, as described in Figure 3. *UBQ10* gene expression was used as a loading control. Values are means  $\pm$  SD of three biological replicates. r.u., Relative units. Different letters above the bars represent significant differences among all the means ( $P < 0.05$ ). [See online article for color version of this figure.]

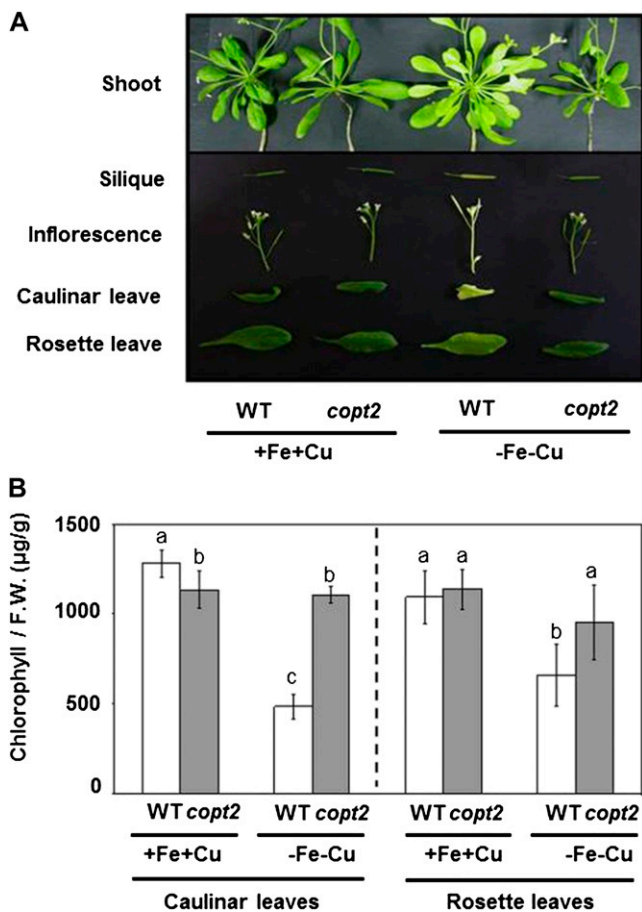


**Figure 6.** Phenotypes of *copt2-1* adult plants grown under Cu and Fe deficiencies. A, Photographs of rosette leaves and aerial part details from the wild type (WT) and the *copt2-1* line grown on the +Fe+Cu and -Fe-Cu media were taken 14 d after treatments. B, Chlorophyll contents of cauline and rosette leaves from the wild-type (white bars) and *copt2* (gray bars) plants shown in A. Values are means  $\pm$  SD of four biological replicates. F.W., Fresh weight. Different letters above the bars represent significant differences ( $P < 0.05$ ) among treatments in each type of leaf.

phenotypes observed in the *copt2-1* line, the Fe and Cu contents from the 7-d-old seedlings grown under the four Fe/Cu conditions described above were determined by inductively coupled plasma mass spectrometry (ICP-MS). No significant differences in Fe content were observed between wild-type and *copt2-1* plants (Fig. 7A). Although a slight decrease in Cu content was detected in the mutant under high Cu (Fig. 7B), *COPT2* was expressed at low levels under these conditions (Fig. 3A), questioning a putative *COPT2* role in Cu uptake from the medium under high Cu. Moreover, no significant differences in Cu content between the wild-type and *copt2-1* plants grown under either hydroponic or Cu deficiency conditions were found in different organs, such as roots, rosette leaves, stems, or inflorescences (data not shown). These results suggest that the total endogenous metal content in seedlings is not responsible for the phenotype of the simultaneous

resistance to Fe and Cu deficiencies displayed by the *copt2-1* line.

#### The Negative Effects of Fe Starvation on Cu Deficiency Responses Are Altered in the *copt2-1* Line

In order to understand the molecular reasons underlying the *copt2-1* phenotype, the mRNA levels of selected genes regulated by Cu deficiency (*COPT1*, *FSD1*, and *CSD2*) were determined by quantitative PCR (qPCR) in 7-d-old wild-type and mutant seedlings grown under the four Fe/Cu conditions described above (Fig. 8). We observed that *COPT1* expression was up-regulated by Cu deficiency in both wild-type and *copt2-1* lines (Fig. 8A, +Fe+Cu versus +Fe-Cu; Sancenón et al., 2003). It is interesting that when Fe was limited (-Fe conditions), no *COPT1* up-regulation was observed in response to Cu deficiency (Fig. 8A, -Fe+Cu versus -Fe-Cu). These results suggest that Fe deficiency negatively affects *COPT1* induction by low Cu in both the wild-type and *copt2-1* lines. To further address this observation, we determined the mRNA levels of Cu-regulated genes *FSD1*

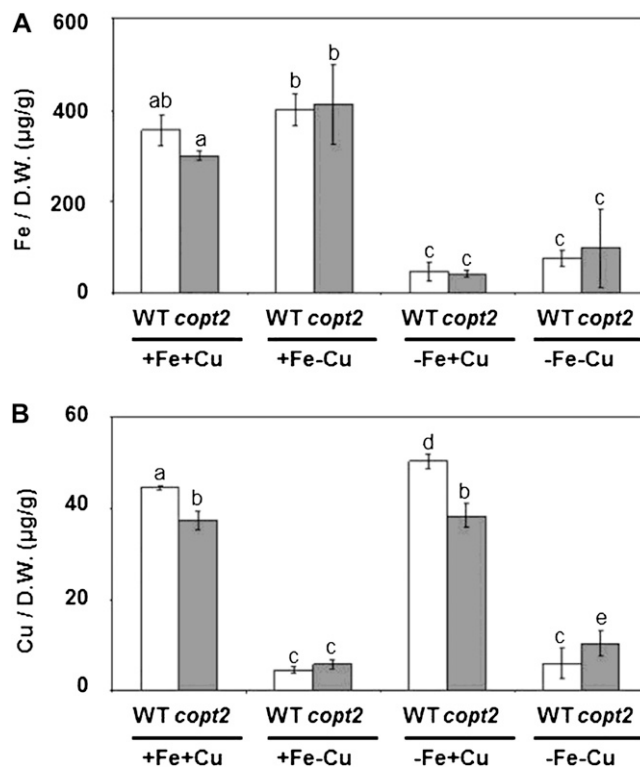


**Figure 7.** Endogenous Fe and Cu contents in wild-type and *copt2-1* seedlings. Fe (A) and Cu (B) contents were measured by ICP-MS from whole 7-d-old wild-type (WT; white bars) and *copt2-1* (gray bars) plants. Seedlings were grown under the same conditions described in Figure 3. Values are means  $\pm$  SD of at least three biological replicates. D.W., Dry weight. Different letters above the bars represent significant differences among all the means ( $P < 0.05$ ).

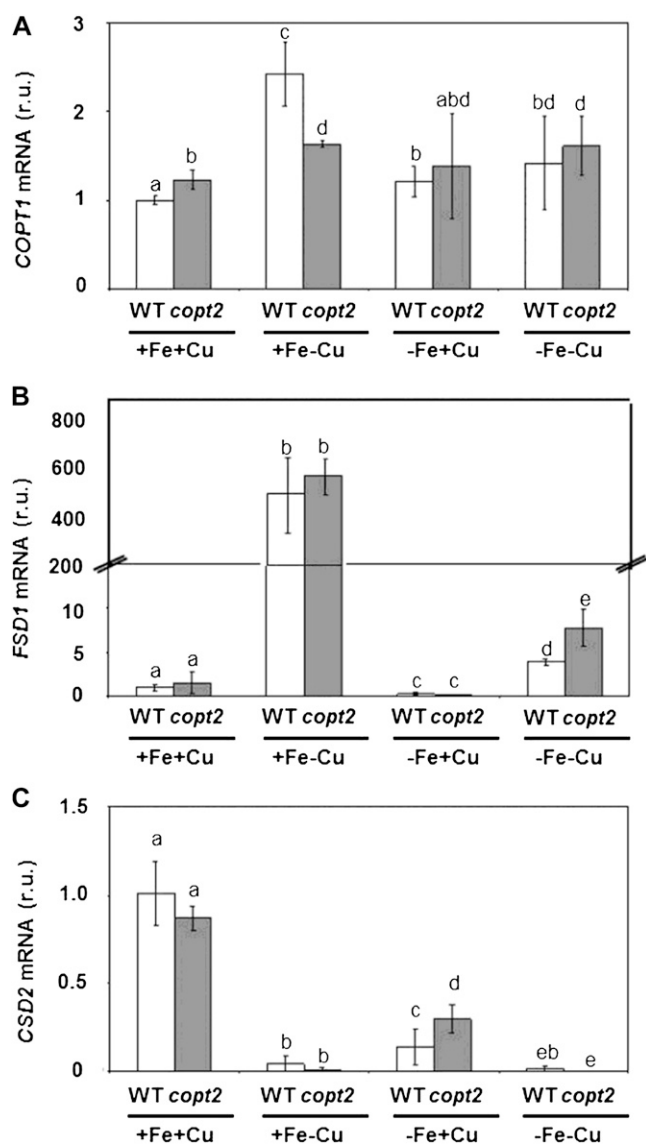


**Figure 8.** Gene expression pattern of Cu deficiency marker genes in *copt2-1* seedlings. Expression analysis is shown for the Cu transporter *COPT1* (A) and the FeSOD and Cu/ZnSOD genes *FSD1* (B) and *CSD2* (C), respectively, by qPCR in wild-type (WT; white bars) and *copt2-1* (gray bars) seedlings, grown under the same conditions described in Figure 3. *UBQ10* gene expression was used as a loading control. Values are means  $\pm$  SD of three biological replicates. r.u., Relative units. Different letters above the bars represent significant differences among all the means ( $P < 0.05$ ).

and *CSD2*, which encode for FeSOD and Cu/ZnSOD, respectively. As Figure 8, B and C, depicts, the *CSD2*/*FSD1* substitution was normally observed with Cu deficiency under Fe-sufficient conditions (+Fe+Cu versus +Fe-Cu). However, when Fe deficiency was imposed, the increased *FSD1* mRNA levels were greatly compromised (Fig. 8B, -Fe+Cu versus -Fe-Cu), and the *copt2-1* line showed a slightly increased *FSD1* expression under Cu and Fe deficiencies (Fig. 8B). To check whether this slight increase in

superoxide dismutase (SOD) expression implies a general enhancement in oxidative stress protection in the *copt2-1* line, SOD activities were measured in gel and no significant differences were found between the wild type and the mutant (Supplemental Fig. S10A). Moreover, when subjected to oxidative treatments, such as hydrogen peroxide (500  $\mu$ M) or paraquat (0.1  $\mu$ M), no phenotypical differences were observed (Supplemental Fig. S10B), indicating that the *copt2-1* line does not show more resistance to general oxidative stress conditions.

Since Fe starvation attenuated the Cu deficiency-induced up-regulation of *COPT1* and *FSD1* (Fig. 8, A and B), we wondered how Cu deficiency could affect plant responses to Fe scarcity. For this purpose, the expression patterns of two well-known Fe deficiency genes, the metalloredutase *FRO2* and the Fe transporter *IRT1*, were analyzed under the four previously assayed Fe/Cu conditions. Although both genes were activated in response to Fe deficiency (Supplemental Fig. S11, A and B, +Fe versus -Fe), as reported previously (Colangelo and Guerinot, 2004), no major differences were observed in the expression of *FRO2* and *IRT1* in *copt2-1* plants (Supplemental Fig. S11).

#### Global Analysis of Gene Expression Changes under Fe and Cu Deficiencies Indicate That *copt2-1* Plants Display Pi Starvation Responses

With the aim of characterizing at the molecular level the causes of enhanced resistance to Fe deficiency and induced chlorosis in the *copt2-1* mutant, a global profiling analysis of gene expression under Fe and Cu deficiency was performed. To that end, wild-type and *copt2-1* seedlings were grown for 7 d under Fe- and Cu-sufficient conditions (+Fe+Cu) and compared with seedlings grown on medium without Fe and Cu (-Fe-Cu). Moreover, medium without Fe (-Fe+Cu) was used as a control for Cu-complemented expression changes in the *copt2-1* line. In order to validate these growth conditions, we previously confirmed by qPCR analysis the expression pattern of two genes previously known to be up-regulated by Cu deficiency, *COPT2* (Sancenón et al., 2003; Fig. 3A; Supplemental Fig. S12A) and *ZIP2*, a ZRT and IRT-like protein2 transporter (Wintz et al., 2003; Supplemental Fig. S12B).

Global profiling analysis of *copt2-1* and wild-type lines was carried out from four biological replicates grown in the three different conditions (+Fe+Cu, -Fe-Cu, and -Fe+Cu). A median  $\log_2$  ratio of 1 (2-fold difference in expression) was used as a cutoff criterion to compare the mutant with the wild type under each condition. We identified 324 differentially expressed genes (Supplemental Tables S1 and S2) distributed in 49 induced (ratio  $> 1$ ) and 275 repressed (ratio  $< 1$ ) genes in the *copt2-1* line in the three growth conditions (Fig. 9A). Repressed genes are more abundant than induced genes in all three conditions. The



condition  $-Fe+Cu$  shows the largest number of genes in which expression is affected. Gene Ontology analysis indicated that repressed genes include those of the abiotic stress and detoxifying processes, maybe reflecting the consequences of dismantling the photosynthetic apparatus taking place in wild-type plants (Supplemental Table S3), which may be delayed in the mutant. Interestingly, a significant percentage (35%) of the induced genes are related to Pi starvation responses based on the literature (Table I). Overrepresentation of this category in all three nutritional conditions indicated a general effect of *COPT2* function in Pi starvation (Supplemental Table S4). The riboregulators *At4*, *IPS1*, and several SPX domain proteins are among the best-known genes induced in

Pi-starved plants, and they have been shown to participate in Pi homeostasis and signaling (Franco-Zorrilla et al., 2007; Duan et al., 2008; Thibaud et al., 2010; Chiou and Lin, 2011). Therefore, *At4* and *SPX1* expression was analyzed in the *copt2-1* line, confirming the microarray results (Fig. 9B). Moreover, these data underscore the intricate interactions between Fe and Pi deficiencies, since whereas *At4* is down-regulated by Fe deficiency in the wild type, *SPX1* expression remains mostly unaffected (Fig. 9B). To check how Cu is implicated in Pi starvation, we grew wild-type and *copt2-1* seedlings in Pi-deficient medium and under different Cu and Fe regimes. As shown in Figure 10, A and B, *copt2-1* displays slightly larger roots than wild-type plants in all growth conditions, indicating a general insensitivity to Pi deficiency. Moreover, the *COPT2* expression pattern remains unaffected under Pi starvation (Fig. 10C). Taken together, our results are compatible with a model where *COPT2* is involved in the antagonistic responses of metals and Pi deficiencies (Fig. 11).

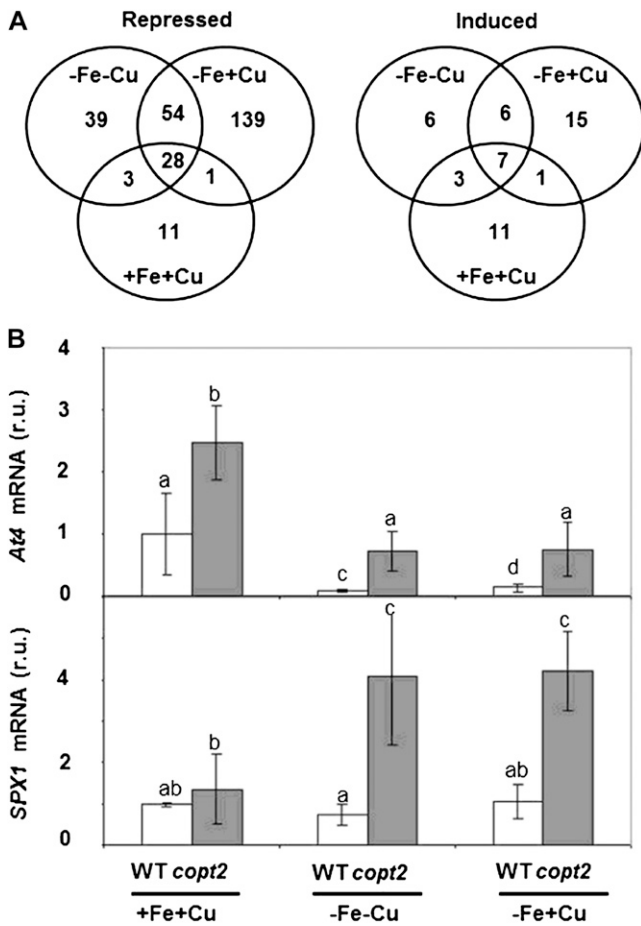


**Figure 9.** Venn diagrams of gene expression changes in wild-type versus *copt2-1* seedlings under different metal statuses. A, Values indicate the number of induced/repressed genes grown under the same conditions described in Figure 3B in *copt2-1* seedlings: control (+Fe+Cu), Fe deficiency ( $-Fe+Cu$ ), or Fe and Cu deficiency ( $-Fe-Cu$ ). B, Expression analysis by qPCR of *At4* and *SPX1* in wild-type (WT; white bars) and *copt2-1* (gray bars) seedlings, as described in A. *UBQ10* gene expression was used as a loading control. Values are means  $\pm$  SD of at least three biological replicates. r.u., Relative units. Different letters above the bars represent significant differences among all the means ( $P < 0.05$ ).

**DISCUSSION**

The conserved family of CTR/COPT proteins mediates high-affinity Cu transport in eukaryotic organisms (for review, see Puig et al., 2002; Kim et al., 2008; Nevitt et al., 2012). Distinct COPT family members have been characterized in Arabidopsis. Whereas COPT1 is a plasma membrane protein that functions in root Cu uptake and pollen development, COPT5 is intracellularly localized and mediates Cu mobilization under severe deficiency conditions (Sancenón et al., 2004; Garcia-Molina et al., 2011; Klaumann et al., 2011). Previous studies have shown that COPT2 is the most similar COPT family protein to COPT1, that both genes fully complement the Cu transport defect of yeast *ctr1Δctr3Δ* mutants, and that they are up-regulated in response to Cu deficiency in an SPL7-dependent manner, probably by SPL7 binding to GTAC motifs in the *COPT1* and *COPT2* promoter regions (Sancenón et al., 2003; Yamasaki et al., 2009; Bernal et al., 2012). Here, we show that, similar to COPT1, the COPT2 protein localizes to the plasma membrane of Arabidopsis cells. Furthermore, both genes display a similar aerial expression pattern under slight Cu-deficient conditions (1/2 MS medium), including expression in cotyledons from young seedlings, trichomes, anthers, and mature pollen (Sancenón et al., 2004). These observations suggest that COPT1 and COPT2 might exhibit a partially redundant function in Cu homeostasis in the aerial part. A notable difference between COPT1 and COPT2 concerns their root expression patterns. *COPT1* is exclusively expressed in primary and secondary root tips (Sancenón et al., 2004), where overexpression activates plasma membrane hydroxyl radical-sensitive calcium and potassium channels and subsequent root apex signaling (Rodrigo-Moreno et al., 2013). However, *COPT2* is expressed in subapical root regions (Fig. 2), where the activation of

**Table 1.** *Pi*-starvation biological process overrepresented in the *copt2-1* line

Common *Pi*-starvation- and *copt2-1*-induced genes compared with the wild type are indicated (Thibaud et al., 2010; asterisks indicate other sources). Munich Information Center for Protein Sequences (MIPS) codes, gene description, gene ontology cellular function, and the microarray values under +Fe+Cu, -Fe-Cu, and -Fe+Cu are indicated. The genes used in qPCR quantitation are in boldface; the genes that are statistically significant with values of less than 1 are italic; and genes that are not statistically significant are indicated as n.s.

MIPS Code	Gene Description	Gene Ontology Cellular Function	+Fe+Cu	-Fe-Cu	-Fe+Cu
At2g32960*	PFA-DSP2	Catalytic activity, phosphatase activity, protein Tyr phosphatase activity	2.524	2.873	2.652
At2g04460	Unknown	Unknown	2.205	2.495	2.300
At5g03545*	<b>At4</b>	Unknown	1.383	1.986	1.855
At5g20150	<b>SPX1</b>	Unknown	1.145	1.309	1.477
At1g73010	PPsPase1	Phosphoric monoester hydrolase activity	1.073	1.222	1.165
At2g11810	MGD3	1,2-Diacylglycerol 3- $\beta$ -galactosyltransferase activity	1.306	1.052	0.738
At5g20790	Unknown	Unknown	<i>0.865</i>	1.811	1.515
At3g09922*	IPS1	Unknown	<i>0.614</i>	1.354	1.469
At1g73220	OCT1	Carbohydrate and carnitine transporter activity	2.067	<i>0.782</i>	<i>0.733</i>
At3g03530	NPC4	Hydrolase and phospholipase C activity	1.112	<i>0.489</i>	<i>0.607</i>
At1g17710	Unknown	Phosphoric monoester hydrolase activity	1.448	1.289	n.s.
At1g08310	Unknown	Galactolipid biosynthetic process, negative regulation of transcription, DNA dependent	1.000	1.441	n.s.
At4g26530*	Unknown	Fru-bisphosphate aldolase activity	1.123	<i>0.219</i>	n.s.
At2g45130	SPX3	Unknown	2.069	n.s.	n.s.
At2g30540	Unknown	Thiol-disulfide exchange intermediate activity	1.039	n.s.	n.s.
At4g11800*	Unknown	Protein Ser/Thr phosphatase activity	n.s.	1.129	n.s.
At1g21980*	PIP5K1	1-Phosphatidylinositol-4-P 5-kinase activity	n.s.	n.s.	1.111

these channels is prevented (Rodrigo-Moreno et al., 2013), suggesting local and specific functions and subsequent signaling events of these transporters in Arabidopsis roots. Moreover, another key difference is the regulation of both genes under Fe deficiency. In low-Cu medium, whereas *COPT1* is down-regulated (Fig. 8A), *COPT2* expression is increased by Fe deficiency (Fig. 3A).

In this sense, it is noteworthy that previous genome-wide expression studies in Fe-deficient roots were mostly performed under low Cu levels (Colangelo and Guerinot, 2004; Buckhout et al., 2009; Yang et al., 2010; Stein and Waters, 2012). These studies have shown that *COPT2* expression is up-regulated in response to Fe deficiency, which has been further corroborated herein (Fig. 3; Supplemental Fig. S5). However, the Fe deficiency-induced *COPT2* expression in roots is abolished by high Cu in medium, although it is still present in shoots (Fig. 3B; Supplemental Fig. S5), suggesting a role for Cu in FIT-mediated responses in Arabidopsis roots. Recently, Waters et al. (2012) reported increased *COPT2* expression in roots but a decrease in rosettes for Fe deficiency under low-Cu conditions. The remaining *COPT2* expression in cotyledons under -Fe+Cu (Fig. 3B; Supplemental Fig. S5) may be attributed to another putative Fe deficiency network that differs from FIT and is not affected by high Cu levels. It is believed that the increase in endogenous Cu levels when Fe is low (Fig. 7B) may occur to favor the cofactor supply to Cu enzymes (e.g. Cu/ZnSOD), which substitute their Fe counterparts (e.g. FeSOD) to optimize the utilization of low Fe available in more important or irreplaceable Fe-dependent functions (Waters et al., 2012).

Surprisingly, parameters indicative of the photosynthetic apparatus status, such as chlorophyll content, are higher in *copt2-1* than in wild-type plants (Figs. 4 and 5), indicating that the absence of *COPT2* expression results in better plant performance, which is more relevant under both metal deficiencies (Supplemental Fig. S9). A putative explanation for this interesting phenotype is based on the observation that *copt2-1* plants display higher *FSD1* mRNA levels than wild-type plants for combined Fe and Cu deficiencies (Fig. 8B). However, a concomitant disadvantageous effect of *COPT2* expression resulting from diminished oxidative protection is not observed in the *copt2-1* line (Supplemental Fig. S10). Instead, the analysis of global expression changes in the *copt2-1* mutant suggests a complex scenario where different cuproproteins and maybe specific COPT-mediated signaling processes could be the basis of the observed phenotype. One of the altered categories in the *copt2-1* line is the response to low Pi, which is mostly independent of the metal status (Fig. 9B; Supplemental Tables S1 and S2). Our results reveal a role of *COPT2*-mediated Cu transport in Pi starvation signaling, which is in agreement with the down-regulated *COPT2* expression observed under Pi starvation conditions (Thibaud et al., 2010). Potential connections between Pi starvation responses and the homeostasis of other ions have been described (Abel, 2011; Chiou and Lin, 2011). Root responses to Pi starvation have been suggested to be an outcome of the complex interactions between Pi and other nutrients, essentially Fe (Svistoonoff et al., 2007; Ward et al., 2008). With simultaneous Fe and Pi deficiencies, a recovery in primary root elongation has been reported (Ward et al., 2008). Our results add Cu homeostasis to

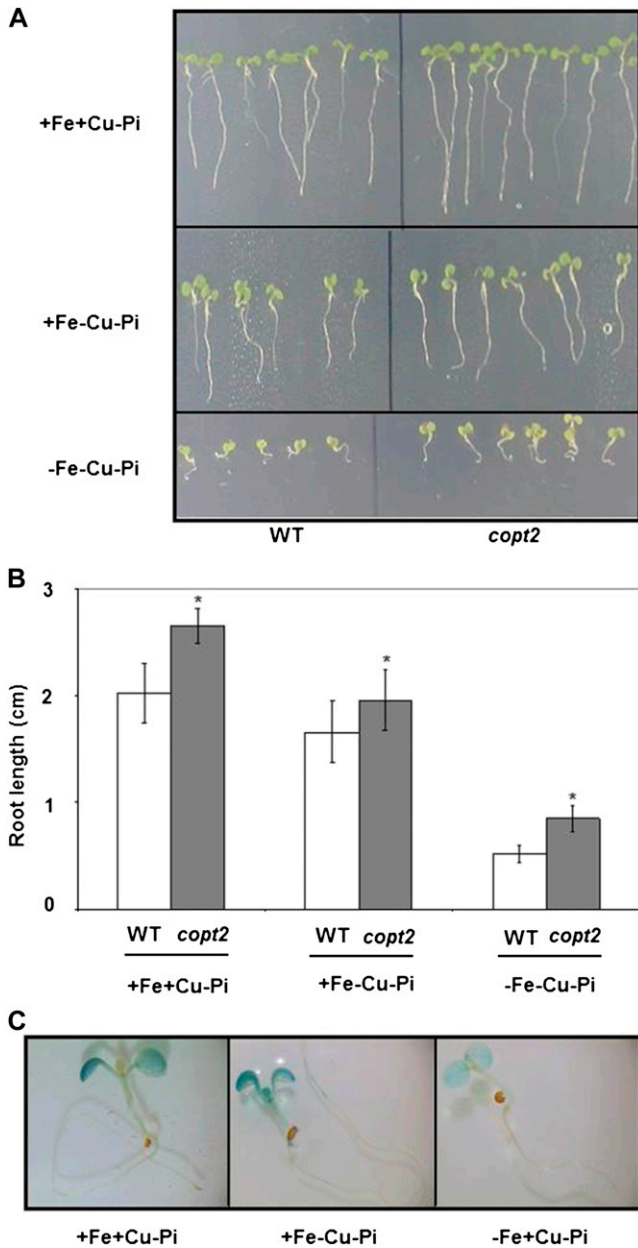


**Figure 10.** Phenotypes of *copt2-1* seedlings grown under Pi, Cu, and Fe deficiencies. **A**, Representative photographs of 7-d-old seedlings from the wild type (WT) and the *copt2-1* line grown under Pi starvation (–Pi) and the conditions described in Figure 3A with regard to Cu deficiency (–Cu) and Cu and Fe deficiencies (–Cu–Fe). **B**, Root lengths from the wild type (white bars) and *copt2* (gray bars) measured in three biological replicates  $\pm$  SD in the samples described in **A**. Asterisks above the bars represent significant differences among all the means ( $P < 0.05$ ) compared with the wild type. **C**, Overnight GUS staining in 7-d-old seedlings from the *PCOPT2:GUS* transgenic line grown under Pi deficiency (+Fe+Cu–Pi), Cu and Pi deficiency (+Fe–Cu–Pi), and Fe and Pi deficiency (–Fe+Cu–Pi). [See online article for color version of this figure.]

those interactions in which Fe deficiency and Pi starvation have antagonistic effects by up-regulating and down-regulating *COPT2* expression, respectively (Figs. 3A and 11; Thibaud et al., 2010).

*COPT2* could participate in Pi sensing by Cu delivery to cuproproteins, such as the multicopper oxidases LPR1 and LPR2 (for low phosphate root), which have been involved in root growth responses to low Pi (Svistonoff et al., 2007). Our results are compatible with a role of *COPT2*-mediated Cu transport in supplying Cu to these enzymes. In this sense, a slight increase in root length is observed in the *copt2-1* line as compared with the wild type under low-Pi conditions (Fig. 10), which is consistent with the phenotype observed in *lpr1* and *lpr2* mutants (Svistonoff et al., 2007). In addition, these data reveal a putative complex *COPT2*-mediated role in Pi starvation systemic signaling, such as *At4* and *SPX1* (named after the yeast Syg1 and Pho81 and human XPR1 proteins) expression (Fig. 9B), which still remains to be elucidated.

A putative explanation for the better maintenance of chlorophylls observed in the mutant can be postulated as an indirect effect through Pi starvation responses. Indeed, under Pi-limiting conditions, plants substitute phosphoglycerolipids by activating the genes for galactolipid biosynthesis (Kobayashi et al., 2009). Monogalactosyldiacylglycerol is an abundant lipid in chloroplast membranes (Shimajima and Ohta, 2011). Mutants affected in monogalactosyldiacylglycerol synthase show reduced chlorophyll content (Jarvis et al., 2000). Changes in lipid composition have

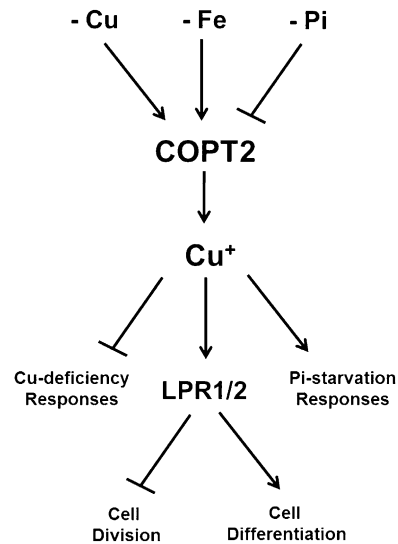


**Figure 11.** Model of the *COPT2*-mediated interactions among Cu and Fe deficiencies and Pi starvation responses. Cu, Fe, and Pi deficiencies display antagonistic effects on *COPT2* expression.  $\text{Cu}^+$  uptake mediated by *COPT2*-attenuated Cu deficiency responses could participate in Cu delivery to low-Pi local sensing and systemic signaling. Local sensing mediated by the multicopper oxidases LPR1 and LPR2 potentiates cell differentiation versus cell division.

already been shown to be involved in Cu deficiency responses in *Chlamydomonas reinhardtii* (Castruita et al., 2011). The genes induced in *copt2-1* plants suggest that phospholipid substitution for galactolipids could take place in the mutant (Table I; Supplemental Tables S2 and S4). Alternatively, a putative COPT2-mediated signaling event could be involved in chlorophyll degradation, and consequently, this process would be retarded in the *copt2-1* line. In agreement with this suggestion, other degradation processes, such as seed protein mobilization, are also inhibited in the mutant (Supplemental Tables S1 and S3). In addition, both the influence of Cu on ethylene perception (Hirayama et al., 1999) and the recently postulated role of a multicopper oxidase in Fe homeostasis (Bernal et al., 2012) also indicate different Cu functions, which could affect plant responses under Fe and Pi starvation (Romera and Alcantara, 1994; Hirsch et al., 2006).

Although more studies will be needed to further ascertain the relevance of COPT2 in these processes, this study opens up novel possibilities to help develop strategies to improve the growth, yield, and nutritional quality of crops under environmental metal deficiencies. Along these lines, recent studies in rice (*Oryza sativa*) implicate certain COPT family members, which are up-regulated by both Cu and Fe deficiency (Yuan et al., 2011), as potential targets for biotechnological improvement.

## MATERIALS AND METHODS

### Plant Growth Conditions and Treatments

Seeds of *Arabidopsis thaliana* (ecotype Columbia-0), were surface sterilized and stratified for 2 d at 4°C and then germinated on 1/2 MS plates either including 1% Suc (Murashige and Skoog, 1962) or supplemented with the indicated concentrations of metal ions. For severe Cu-deficient conditions, the 1/2 MS was supplemented with 100  $\mu\text{M}$  bathocuproinedisulfonic acid disodium. In order to know the effects of both Cu and Fe deficiencies in plants, the components of the 1/2 MS were prepared separately according to the following conditions: macronutrients (10 mM  $\text{NH}_4\text{NO}_3$ , 9.4 mM  $\text{KNO}_3$ , 0.37 mM  $\text{MgSO}_4 \cdot 7\text{H}_2\text{O}$ , 0.62 mM  $\text{KH}_2\text{PO}_4$ , and 1.13 mM  $\text{CaCl}_2$ ), micronutrients (50  $\mu\text{M}$   $\text{H}_3\text{BO}_3$ , 36.6  $\mu\text{M}$   $\text{MnSO}_4 \cdot \text{H}_2\text{O}$ , 15  $\mu\text{M}$   $\text{ZnSO}_4 \cdot 7\text{H}_2\text{O}$ , 0.57  $\mu\text{M}$   $\text{NaMoO}_4 \cdot 2\text{H}_2\text{O}$ , and 0.05  $\mu\text{M}$   $\text{CoCl}_2 \cdot 6\text{H}_2\text{O}$ ), 50  $\mu\text{M}$  Fe-EDTA, 0.25 mM potassium iodide, 1  $\mu\text{M}$   $\text{CuSO}_4 \cdot 5\text{H}_2\text{O}$ , 0.05% MES, 1% Suc, and 0.8% phytoagar, pH 5.7 to 5.8. Seven-day-old seedlings were grown in Fe- and Cu-sufficient medium (+Fe+Cu), Fe-sufficient and Cu-deficient medium (+Fe–Cu), Fe-deficient and Cu-sufficient medium (–Fe+Cu), and Fe- and Cu-deficient medium (–Fe–Cu). Cu-excess medium was supplemented with 10  $\mu\text{M}$   $\text{CuSO}_4 \cdot 5\text{H}_2\text{O}$ . Fe-deficient medium was supplemented with 300  $\mu\text{M}$  ferrozine. With the Pi-deficient medium,  $\text{KH}_2\text{PO}_4$  was not included in the macronutrient solution. To study sensitivity to others stresses, seedlings were grown in paraquat and hydrogen peroxide solution (0.1 and 500  $\mu\text{M}$ , respectively). Seedlings were grown for 7 d with a 12-h photoperiod (65  $\mu\text{mol m}^{-2}$  cool-white fluorescent light) at a 23°C/16°C temperature cycle. Hydroponic cultures were performed in the same photoperiod conditions from three- to four-true-leaf seedlings grown in commercial soil, which were transferred to black boxes containing standard Hoagland solution (0.1 $\times$ ), pH 5.8, as described by Hermans et al. (2005). After a 14-d adaptation, the –Fe–Cu treatment (corresponding to Hoagland medium without Cu and Fe sources) commenced. Media were changed weekly for 4 to 5 weeks. The chlorophyll content of the *Arabidopsis* seedlings and leaves from adult plants was determined by the trichlorometric method (Parsons and Strickland, 1962). Root length was measured using ImageJ 1.42q software (<http://rsb.info.nih.gov/ij>).

### Functional Complementation Assays in Yeast

The yeast (*Saccharomyces cerevisiae*) *ctr1 $\Delta$ ctr3 $\Delta$*  mutant strain was transformed with p426GPD or with a vector containing *COPT1*, *COPT2*, or *COPT2:GFP* and was assayed for growth on Glc (1% yeast extract, 2% bacto-peptone, and 2% Glc), glycerol (1% yeast extract, 2% bacto-peptone, 2% ethanol, and 3% glycerol), and glycerol + Cu (1% yeast extract, 2% bacto-peptone, 2% ethanol, 3% glycerol, and 100  $\mu\text{M}$   $\text{CuSO}_4$ ) media solidified with 1.5% agar (Puig et al., 2002).

### Metal Accumulation Measurements

Fresh *Arabidopsis* material was dried at 65°C for 2 d and digested with 65% (v/v)  $\text{HNO}_3$  at 80°C to 90°C. Digested samples were then diluted with Millipore water (Purelab Ultra), and Cu and Fe contents were determined by ICP-MS at the Servei Central d'Instrumentació Científica (Universitat Jaume I).

### SOD Activity Assay

Plant material was homogenized in an equal volume of ice-cold grinding buffer (50 mM potassium phosphate, pH 7.4, 0.1% bovine serum albumin [BSA], 0.1% ascorbate, 0.05%  $\beta$ -mercaptoethanol, and 0.2% Triton X-100) and was clarified by centrifugation at 14,000 rpm for 15 min. Total protein was measured by the protein-dye binding assay (Bradford, 1976) with the Bio-Rad Protein Assay reagent. Samples (20  $\mu\text{g}$ ) were separated on a nondenaturing 12.5% polyacrylamide gel at 100 V for 3 to 4 h. SOD activity was detected on these gels using the in situ staining technique of Beauchamp and Fridovich (1971). Briefly, the gel was kept in 1 mg  $\text{mL}^{-1}$  nitroblue tetrazolium for 10 min in the dark and then in developing buffer (33 mM potassium phosphate, pH 7.8, 28  $\mu\text{M}$  riboflavin, and 28 mM *N,N,N',N'*-tetramethylethylenediamine) for another 20-min period before exposure to light.

### Plasmid Constructs

The entire *COPT2* open reading frame was obtained by PCR using the following specific primers: *COPT2-Sall-F* (5'-CATGTCGACATCATGGATCATGATCACATGCAT-3') and *COPT2-NcoI-R* (5'-TCTCCATGGTACAACGCCCTGAAGACGGCGGAA-3'). The *COPT2 C* terminus was fused in frame to the *GFP* with the *CaMV35S* promoter through its insertion into transient expression vector P35S $\Omega$ s:*GFP(S65T)* (Miras et al., 2002). *COPT2-GFP*, obtained from the previous construct by PCR using the specific primers *COPT2-HindIII-F* (5'-CATAAGCTTATGGATCATGATCACATGCAT-3') and *GFP-R-SalI* (5'-CATGTCGACTTACTGTACAGCTCGCCAT-3') was cloned into the p426GDP plasmid for the yeast functionality assay. Plasmids p426GDP-*COPT1* and p426GDP-*COPT2* were described by Sancenón et al. (2003). The *uidA* coding sequence and 1,248 bp from the *COPT2* transcription start site (*PCOPT2*; arrows in Supplemental Fig. S4) were amplified and cloned into the pFP101 plasmid (Bensmihen et al., 2005) without its *CaMV35S* promoter to obtain the *PCOPT2:GUS* construct, used to determine the *COPT2* spatial expression pattern by a GUS assay. A PCR product containing 1,248 bp of the *PCOPT2* and the entire *COPT2* coding sequence was cloned into the pFP101 vector and introduced into the *copt2-1* line by floral dipping (Clough and Bent 1998). Homozygous transgenic plants (*PCOPT2:COPT2*) were selected based on seed fluorescence. The entire *COPT2* coding sequence was tagged with the human influenza virus HA epitope with the specific primers *COPT2-XbaI-F* (5'-CATTCTAGAATGGATCATGATCACATGCAT-3') and *COPT2HA-SalI-R* (5'-ATGTCGACTCAAGCATAATCTGGAACATCGTATGGATAACAAACGCAGCCTGAAGACGGCGGAA-3') and cloned into the pFP101 vector. Transgenic lines were selected based on the fluorescence of the seeds.

### Computer-Assisted Sequence Analyses

The hydrophobic profile of the *COPT2* protein was obtained by the TMHMM application ([www.cbs.dtu.dk/services](http://www.cbs.dtu.dk/services)). The theoretical analysis of the promoter sequences was performed with the PLACE Web Signal Scan ([www.dna.affrc.go.jp/PLACE/signalscan.html](http://www.dna.affrc.go.jp/PLACE/signalscan.html)) and Patmatch from The *Arabidopsis* Information Resource ([www.arabidopsis.org](http://www.arabidopsis.org)).

### Subcellular Localization of the GFP Fusion Proteins

The *Arabidopsis* protoplasts from fresh leaf tissue of 30-d-old plants grown in soil were transiently transformed with *COPT2-GFP* as described previously

(Abdel-Ghany et al., 2005). After 16 h under continuous light at 23°C in the wash solution, protoplasts were incubated with FM4-64 dye (Invitrogen) at a concentration of 50  $\mu\text{M}$  for 15 min at 4°C before analyzing. Confocal images were obtained using fluorescence confocal microscope TCS SP, vertical (DM-R; Leica), equipped with argon ion (458 and 488 nm), helium-neon I (543 nm), and helium-neon II (633 nm) excitation laser systems and a 40 $\times$  to 60 $\times$  objective lens. Fluorescence signals were detected at 500 to 530 nm for GFP, 650 to 750 nm for chlorophyll, and 560 to 650 nm for FM4-64 after exciting at 488, 633, and 543 nm, respectively.

## Immunohistochemical Techniques and Microscopy

Samples of Arabidopsis leaves were fixed in Karnovsky reagent. They were dehydrated in a successive ethanol series (20%, 40%, 60%, 80%, 95%, and 100%) and embedded in polyethylene glycol for fluorescence microscopy. Semithin sections (2  $\mu\text{m}$ ) were placed on slides and rehydrated with xylene and a successive ethanol series (100%, 95%, 70%, and 0%), washed with PBSII (PBSI [137 mM NaCl, 2.7 mM KCl, 9 mM  $\text{Na}_2\text{HPO}_4$ , and 1.5 mM  $\text{KH}_2\text{PO}_4$ , pH 7.2] + 0.1% BSA and 0.05%  $\text{Na}_2\text{N}_3$ ), and dried. Slides were blocked in PBSII with 2% BSA and 1% powder milk for 20 min and dried. Then, they were labeled overnight at 4°C and in humidity with rat monoclonal antibody to the HA epitope (clone 3F10; Roche) diluted 1:50 in PBSII. Subsequently, they were washed with PBSI, blocked in PBSII with 2% BSA and 1% powder milk for 20 min, and dried. Then, an anti-rat IgG antibody conjugated with AlexaFluor546 (Molecular Probes) diluted 1:500 with 0.1 M Gly was used for 1 to 4 h at 4°C in humidity and darkness. Slides were then washed with PBSI and stained with 1  $\mu\text{g mL}^{-1}$  4',6-diamino-phenylindole in PBSI for 5 min. Finally, the slides were washed with PBSI and mounted in Citifluor. The fluorescence of immunolabeled COPT2-HA and of 4',6-diamino-phenylindole-stained nuclei was visualized with a fluorescence microscope (Axioskop 2; Zeiss) using the appropriate filter combinations. Micrographs were taken by a SPOT camera (Diagnostic Instruments) and were processed through the Photoshop program (Adobe Systems).

## Protein Analysis by Western Blot

Crude extracts from wild-type and *copt2-1* Arabidopsis leaves grown on plates were obtained, and the amount of protein was determined by bicinchoninic acid with the BCA Protein Assay Kit (Thermo). Next, 40  $\mu\text{g}$  of protein was analyzed by SDS-PAGE, transferred to a nitrocellulose membrane, and blotted with an antibody against plastocyanin (Agrisera). Coomassie blue staining was used as a loading control.

## GUS Expression Analyses

Assays were performed as described (Jefferson et al., 1987). Briefly, the seedlings and organs from the adult *PCOPT2::GUS* plants were embedded with the substrate solution [100 mM  $\text{NaPO}_4$ , pH 7.2, 0.5 mM  $\text{K}_3\text{Fe}(\text{CN})_6$ , 0.5 mM  $\text{K}_4\text{Fe}(\text{CN})_6$ , 0.1% (v/v) Triton X-100, 0.5 mM 5-bromo-4-chloro-3-indolyl- $\beta$ -D-glucuronide (AppliChem), and 10 mM EDTA, pH 7.2]. Reactions took place at 37°C and were stopped with ethanol (70%).

## *copt2-1* Mutant Line Analyses and Complementation

The Arabidopsis T-DNA insertion line AL770147 was obtained from the GABI-Kat Project. Plants were self-pollinated, and a homozygous mutant was obtained (denoted the *copt2-1* line). The COPT2-LB (F) and COPT2-RB (R) primers were used to amplify the wild-type alleles, whereas the COPT2-LB (F) and GKAT-PCR (S) primers amplified the inserted alleles in the *copt2-1* line (Supplemental Table S6). The location of the T-DNA insert was obtained by PCR amplification and sequencing. Several independent lines obtained from different Arabidopsis databases were checked, but none carried a T-DNA insertion in the coding region, and the *copt2-1* line was the closest insertion to the COPT2 coding sequence found among the lines analyzed. A PCR fragment containing *PCOPT2::COPT2* in frame with the *GFP* reporter gene was cloned into the pFP101 plasmid and introduced in the *copt2-1* line by floral dipping to generate a complemented mutant line.

## Microarrays and Bioinformatics

Four biological replicates (7-d-old seedlings of wild-type and *copt2-1* plants grown in a 12-h-light/12-h-dark photoperiod) were obtained for each

treatment (+Fe+Cu, -Fe+Cu, and -Fe-Cu). Fe-deficient medium was supplemented with 300  $\mu\text{M}$  ferrozine. Total RNA was isolated using the RNeasy Plant Mini Kit (Qiagen), and antisense RNA was amplified using the MessageAmp II aRNA Amplification kit (Ambion). Long oligonucleotide microarrays were provided by Dr. David Galbraith (University of Arizona; <http://www.ag.arizona.edu/microarray/>). The hybridization and analysis were performed as described elsewhere (Bueso et al., 2007). The expression values ( $\log_2$ ) were obtained using the GenePix Pro 6.0 microarray analysis software (Molecular Devices) and normalized with GenePix Pro 6.0 and Acuity 4.0 software (Molecular Devices). Differential genes were identified with significance analysis of microarray (Tusher et al., 2001) with a false discovery rate of less than 6% and 2-fold change ( $\log_2 \leq |1|$ ). Biological processes were identified with the Gene Ontology annotation (Ashburner et al., 2000), performed with GeneCodis2.0 (<http://genecodis.dacya.ucm.es/>; Carmona-Saez et al., 2007; Nogales-Cadenas et al., 2009) programs (Table 1). The total microarray differentially regulated genes are shown in Supplemental Tables S1 and S2. The microarray raw data were deposited in the National Center for Biotechnology Information Gene Expression Omnibus (Edgar et al., 2002) and are accessible through accession number GSE42642.

## Gene Expression by Semiquantitative and Real-Time qPCR

Total Arabidopsis RNA was extracted with Trizol Reagent (Ambion), and reverse transcription-PCR was performed with SuperScript II (Invitrogen), as described previously (Andrés-Colás et al., 2006). RNA was quantified by UV spectrophotometry; its integrity was visually assessed on ethidium bromide-stained agarose gels and was treated with DNase I Amp Grade (Invitrogen). Semiquantitative PCR was carried out with specific oligonucleotides for *ACT1* and *COPT2* (Supplemental Table S6). Real-time qPCR was carried out with SYBR-Green qPCR Super-Mix-UDG with ROX (Invitrogen), and the specific primers detailed in Supplemental Table S6 were used in the CFX96 Touch Real Time PCR Detection System (Bio-Rad) with one cycle of 95°C for 2 min and 40 cycles consisting in 95°C for 30 s and 60°C for 30 s. Values were normalized to the *UBQ10* mRNA levels, and in control conditions the wild type was used as a reference.

## Statistical Analysis

Statistical analysis of relative expression was performed by comparing the relative expression of the genes (reverse transcription PCR) based on the pairwise fixed reallocation randomization test ( $P < 0.05$ ; Pfaffl et al., 2002); for the remaining parameters, it was carried out using two-way ANOVA with the means compared by the Duncan test ( $P \leq 0.05$ ) using the InfoStat software, version 2008 (<http://www.infostat.com.ar>).

Sequence data from this article can be found in the GenBank/EMBL data libraries under accession number At3g46900.

## Supplemental Data

- The following materials are available in the online version of this article.
- Supplemental Figure S1.** COPT2 protein sequence and topology.
  - Supplemental Figure S2.** COPT2 subcellular localization in Arabidopsis COPT2:HA plants.
  - Supplemental Figure S3.** Comparative COPT1 and COPT2 characteristics.
  - Supplemental Figure S4.** Theoretical cis-elements in the COPT2 promoter region.
  - Supplemental Figure S5.** The COPT2 expression pattern in Arabidopsis PCOPT2:GUS transgenic plants under different Cu content.
  - Supplemental Figure S6.** The COPT2 gene expression dramatically diminished in the Arabidopsis *copt2-1* line.
  - Supplemental Figure S7.** Fresh weight and the *LHCB1.1* gene expression in the *copt2-1* seedlings.
  - Supplemental Figure S8.** Plastocyanin content of the *copt2-1* adult plants grown under Cu and Fe deficiencies.

**Supplemental Figure S9.** Phenotype of the siliques from the *copt2-1* mutant plants.

**Supplemental Figure S10.** SODs activity and phenotype of *copt2-1* seedlings grown under several oxidative stresses.

**Supplemental Figure S11.** The gene expression pattern of the Fe-deficiency marker genes in *copt2-1* mutant seedlings.

**Supplemental Figure S12.** The gene expression pattern in *copt2-1* seedlings.

**Supplemental Table S1.** Differential genes repressed in *copt2-1* seedlings.

**Supplemental Table S2.** Differential genes induced in *copt2-1* seedlings.

**Supplemental Table S3.** Biological processes overrepresented in the differential genes repressed in *copt2-1* seedlings.

**Supplemental Table S4.** Biological processes overrepresented in the differential genes induced in *copt2-1* seedlings.

**Supplemental Table S5.** Oligonucleotides used in the qPCR reactions.

**Supplemental Table S6.** Oligonucleotides used in the semiquantitative PCR reactions.

## ACKNOWLEDGMENTS

We thank the Servei Central de Suport a la Investigació Experimental (Universitat de València) for sequencing and confocal microscopy services. We are grateful to Dr. Marinus Pilon for the GFP plasmid and to Dr. Toshiharu Shikanai for the *spl7* mutant. Finally, we thank Drs. Amparo Sanz and Javier Paz-Ares for critically reading the manuscript.

Received December 12, 2012; accepted March 12, 2013; published March 13, 2013.

## LITERATURE CITED

- Abdel-Ghany SE, Müller-Moulé P, Niyogi KK, Pilon M, Shikanai T (2005) Two P-type ATPases are required for copper delivery in *Arabidopsis thaliana* chloroplasts. *Plant Cell* **17**: 1233–1251
- Abel S (2011) Phosphate sensing in root development. *Curr Opin Plant Biol* **14**: 303–309
- Aller SG, Eng ET, De Feo CJ, Unger VM (2004) Eukaryotic CTR copper uptake transporters require two faces of the third transmembrane domain for helix packing, oligomerization, and function. *J Biol Chem* **279**: 53435–53441
- Andrés-Colás N, Perea-García A, Puig S, Peñarrubia L (2010) Deregulated copper transport affects *Arabidopsis* development especially in the absence of environmental cycles. *Plant Physiol* **153**: 170–184
- Andrés-Colás N, Sancenón V, Rodríguez-Navarro S, Mayo S, Thiele DJ, Ecker JR, Puig S, Peñarrubia L (2006) The *Arabidopsis* heavy metal P-type ATPase HMA5 interacts with metallochaperones and functions in copper detoxification of roots. *Plant J* **45**: 225–236
- Ashburner M, Ball CA, Blake JA, Botstein D, Butler H, Cherry JM, Davis AP, Dolinski K, Dwight SS, Eppig JT, et al (2000) Gene Ontology: tool for the unification of biology. *Nat Genet* **25**: 25–29
- Beauchamp C, Fridovich I (1971) Superoxide dismutase: improved assays and an assay applicable to acrylamide gels. *Anal Biochem* **44**: 276–287
- Bensmihen S, Giraudat J, Parcy F (2005) Characterization of three homologous basic leucine zipper transcription factors (bZIP) of the ABI5 family during *Arabidopsis thaliana* embryo maturation. *J Exp Bot* **56**: 597–603
- Bernal M, Casero D, Singh V, Wilson GT, Grande A, Yang H, Dodani SC, Pellegrini M, Huijser P, Connolly EL, et al (2012) Transcriptome sequencing identifies SPL7-regulated copper acquisition genes FRO4/FRO5 and the copper dependence of iron homeostasis in *Arabidopsis*. *Plant Cell* **24**: 738–761
- Birkenbihl RP, Jach G, Saedler H, Huijser P (2005) Functional dissection of the plant-specific SBP-domain: overlap of the DNA-binding and nuclear localization domains. *J Mol Biol* **352**: 585–596
- Bradford MM (1976) A rapid and sensitive method for the quantitation of microgram quantities of protein utilizing the principle of protein-dye binding. *Anal Biochem* **72**: 248–254
- Buckhout TJ, Yang TJ, Schmidt W (2009) Early iron-deficiency-induced transcriptional changes in *Arabidopsis* roots as revealed by microarray analyses. *BMC Genomics* **10**: 147–163
- Bueso E, Alejandro S, Carbonell P, Perez-Amador MA, Fayos J, Bellés JM, Rodríguez PL, Serrano R (2007) The lithium tolerance of the *Arabidopsis* *cat2* mutant reveals a cross-talk between oxidative stress and ethylene. *Plant J* **52**: 1052–1065
- Burkhead JL, Reynolds KA, Abdel-Ghany SE, Cochu CM, Pilon M (2009) Copper homeostasis. *New Phytol* **182**: 799–816
- Carmona-Saez P, Chagoyen M, Tirado F, Carazo JM, Pascual-Montano A (2007) GENECODIS: a Web-based tool for finding significant concurrent annotations in gene lists. *Genome Biol* **8**: R3
- Castruita M, Casero D, Karpowicz SJ, Kropat J, Vieler A, Hsieh SI, Yan W, Cokus S, Loo JA, Benning C, et al (2011) Systems biology approach in *Chlamydomonas* reveals connections between copper nutrition and multiple metabolic steps. *Plant Cell* **23**: 1273–1292
- Chiou TJ, Lin SI (2011) Signaling network in sensing phosphate availability in plants. *Annu Rev Plant Biol* **62**: 185–206
- Clough SJ, Bent AF (1998) Floral dip: a simplified method for *Agrobacterium*-mediated transformation of *Arabidopsis thaliana*. *Plant J* **16**: 735–743
- Colangelo EP, Guerinot ML (2004) The essential basic helix-loop-helix protein FIT1 is required for the iron deficiency response. *Plant Cell* **16**: 3400–3412
- Crichton RR, Pierre JL (2001) Old iron, young copper: from Mars to Venus. *Biometals* **14**: 99–112
- del Pozo T, Cambiazo V, González M (2010) Gene expression profiling analysis of copper homeostasis in *Arabidopsis thaliana*. *Biochem Biophys Res Commun* **393**: 248–252
- Duan K, Yi K, Dang L, Huang H, Wu W, Wu P (2008) Characterization of a sub-family of *Arabidopsis* genes with the SPX domain reveals their diverse functions in plant tolerance to phosphorus starvation. *Plant J* **54**: 965–975
- Edgar R, Domrachev M, Lash AE (2002) Gene Expression Omnibus: NCBI gene expression and hybridization array data repository. *Nucleic Acids Res* **30**: 207–210
- Franco-Zorrilla JM, Valli A, Todesco M, Mateos I, Puga MI, Rubio-Somoza I, Leyva A, Weigel D, García JA, Paz-Ares J (2007) Target mimicry provides a new mechanism for regulation of microRNA activity. *Nat Genet* **39**: 1033–1037
- García-Molina A, Andrés-Colás N, Perea-García A, Del Valle-Tascón S, Peñarrubia L, Puig S (2011) The intracellular *Arabidopsis* COPT5 transport protein is required for photosynthetic electron transport under severe copper deficiency. *Plant J* **65**: 848–860
- Guerinot ML (2000) The ZIP family of metal transporters. *Biochim Biophys Acta* **1465**: 190–198
- Hartmann U, Sagasser M, Mehrtens F, Stracke R, Weisshaar B (2005) Differential combinatorial interactions of cis-acting elements recognized by R2R3-MYB, BZIP, and BHLH factors control light-responsive and tissue-specific activation of phenylpropanoid biosynthesis genes. *Plant Mol Biol* **57**: 155–171
- Hermans C, Bourgis F, Faucher M, Strasser RJ, Delrot S, Verbruggen N (2005) Magnesium deficiency in sugar beets alters sugar partitioning and phloem loading in young mature leaves. *Planta* **220**: 541–549
- Hindt MN, Guerinot ML (2012) Getting a sense for signals: regulation of the plant iron deficiency response. *Biochim Biophys Acta* **1823**: 1521–1530
- Hirayama T, Kieber JJ, Hirayama N, Kogan M, Guzman P, Nourizadeh S, Alonso JM, Dailey WP, Dancis A, Ecker JR (1999) RESPONSIVE-TO-ANTAGONIST1, a Menkes/Wilson disease-related copper transporter, is required for ethylene signaling in *Arabidopsis*. *Cell* **97**: 383–393
- Hirsch J, Marin E, Floriani M, Chiarenza S, Richaud P, Nussaume L, Thibaud MC (2006) Phosphate deficiency promotes modification of iron distribution in *Arabidopsis* plants. *Biochimie* **88**: 1767–1771
- Ivanov R, Brumbarova T, Bauer P (2012) Fitting into the harsh reality: regulation of iron-deficiency responses in dicotyledonous plants. *Mol Plant* **5**: 27–42
- Jarvis P, Dörmann P, Peto CA, Lutes J, Benning C, Chory J (2000) Galactolipid deficiency and abnormal chloroplast development in the *Arabidopsis* MGD synthase 1 mutant. *Proc Natl Acad Sci USA* **97**: 8175–8179
- Jefferson RA, Kavanagh TA, Bevan MW (1987) GUS fusions: beta-glucuronidase as a sensitive and versatile gene fusion marker in higher plants. *EMBO J* **6**: 3901–3907

- Jeong J, Guerinot ML (2009) Homing in on iron homeostasis in plants. *Trends Plant Sci* **14**: 280–285
- Kampfenkel K, Kushnir S, Babychuk E, Inzé D, Van Montagu M (1995) Molecular characterization of a putative *Arabidopsis thaliana* copper transporter and its yeast homologue. *J Biol Chem* **270**: 28479–28486
- Kim BE, Nevitt T, Thiele DJ (2008) Mechanisms for copper acquisition, distribution and regulation. *Nat Chem Biol* **4**: 176–185
- Klaumann S, Nickolaus SD, Fürst SH, Starck S, Schneider S, Ekkehard Neuhaus H, Trentmann O (2011) The tonoplast copper transporter COPT5 acts as an exporter and is required for interorgan allocation of copper in *Arabidopsis thaliana*. *New Phytol* **192**: 393–404
- Kobayashi K, Awai K, Nakamura M, Nagatani A, Masuda T, Ohta H (2009) Type-B monogalactosyldiacylglycerol synthases are involved in phosphate starvation-induced lipid remodeling, and are crucial for low-phosphate adaptation. *Plant J* **57**: 322–331
- Liao H, Rubio G, Yan X, Cao A, Brown KM, Lynch JP (2001) Effect of phosphorus availability on basal root shallowness in common bean. *Plant Soil* **232**: 69–79
- Märschner H (2002) *Mineral Nutrition in Higher Plants*. Academic Press, London
- Miras S, Salvi D, Ferro M, Grunwald D, Garin J, Joyard J, Rolland N (2002) Non-canonical transit peptide for import into the chloroplast. *J Biol Chem* **277**: 47770–47778
- Misson J, Raghothama KG, Jain A, Jouhet J, Block MA, Bligny R, Ortet P, Creff A, Somerville S, Rolland N, et al (2005) A genome-wide transcriptional analysis using *Arabidopsis thaliana* Affymetrix gene chips determined plant responses to phosphate deprivation. *Proc Natl Acad Sci USA* **102**: 11934–11939
- Murashige T, Skoog F (1962) A revised medium for rapid growth and bioassays with tobacco tissue culture. *Physiol Plant* **15**: 473–497
- Nevitt T, Ohrvik H, Thiele DJ (2012) Charting the travels of copper in eukaryotes from yeast to mammals. *Biochim Biophys Acta* **1823**: 1580–1593
- Nogales-Cadenas R, Carmona-Saez P, Vazquez M, Vicente C, Yang X, Tirado F, Carazo JM, Pascual-Montano A (2009) GeneCodis: interpreting gene lists through enrichment analysis and integration of diverse biological information. *Nucleic Acids Res* **37**: W317–W322
- Palmer CM, Guerinot ML (2009) Facing the challenges of Cu, Fe and Zn homeostasis in plants. *Nat Chem Biol* **5**: 333–340
- Parsons TR, Strickland JD (1962) Oceanic detritus. *Science* **136**: 313–314
- Peñarrubia L, Andrés-Colás N, Moreno J, Puig S (2010) Regulation of copper transport in *Arabidopsis thaliana*: a biochemical oscillator? *J Biol Inorg Chem* **15**: 29–36
- Pfaffl MW, Horgan GW, Dempfle L (2002) Relative expression software tool (REST) for group-wise comparison and statistical analysis of relative expression results in real-time PCR. *Nucleic Acids Res* **30**: e36
- Pilon M, Cohu CM, Ravet K, Abdel-Ghany SE, Gaymard F (2009) Essential transition metal homeostasis in plants. *Curr Opin Plant Biol* **12**: 347–357
- Puig S, Andrés-Colás N, García-Molina A, Peñarrubia L (2007) Copper and iron homeostasis in *Arabidopsis*: responses to metal deficiencies, interactions and biotechnological applications. *Plant Cell Environ* **30**: 271–290
- Puig S, Lee J, Lau M, Thiele DJ (2002) Biochemical and genetic analyses of yeast and human high affinity copper transporters suggest a conserved mechanism for copper uptake. *J Biol Chem* **277**: 26021–26030
- Puig S, Peñarrubia L (2009) Placing metal micronutrients in context: transport and distribution in plants. *Curr Opin Plant Biol* **12**: 299–306
- Raghothama KG (1999) Phosphate acquisition. *Annu Rev Plant Physiol Plant Mol Biol* **50**: 665–693
- Rodrigo-Moreno A, Andrés-Colás N, Poschenrieder C, Gunsé B, Peñarrubia L, Shabala S (2013) Calcium- and potassium-permeable plasma membrane transporters are activated by copper in *Arabidopsis* root tips: linking copper transport with cytosolic hydroxyl radical production. *Plant Cell Environ* **36**: 844–855
- Romera FJ, Alcantara E (1994) Iron-deficiency stress responses in cucumber (*Cucumis sativus* L.) roots (a possible role for ethylene?). *Plant Physiol* **105**: 1133–1138
- Sancenón V, Puig S, Mateu-Andrés I, Dorcey E, Thiele DJ, Peñarrubia L (2004) The *Arabidopsis* copper transporter COPT1 functions in root elongation and pollen development. *J Biol Chem* **279**: 15348–15355
- Sancenón V, Puig S, Mira H, Thiele DJ, Peñarrubia L (2003) Identification of a copper transporter family in *Arabidopsis thaliana*. *Plant Mol Biol* **51**: 577–587
- Shimajima M, Ohta H (2011) Critical regulation of galactolipid synthesis controls membrane differentiation and remodeling in distinct plant organs and following environmental changes. *Prog Lipid Res* **50**: 258–266
- Stein RJ, Waters BM (2012) Use of natural variation reveals core genes in the transcriptome of iron-deficient *Arabidopsis thaliana* roots. *J Exp Bot* **63**: 1039–1055
- Svistonoff S, Creff A, Reymond M, Sigoillot-Claude C, Ricaud L, Blanchet A, Nussaume L, Desnos T (2007) Root tip contact with low-phosphate media reprograms plant root architecture. *Nat Genet* **39**: 792–796
- Thibaud MC, Arrighi JF, Bayle V, Chiarenza S, Creff A, Bustos R, Paz-Ares J, Poirier Y, Nussaume L (2010) Dissection of local and systemic transcriptional responses to phosphate starvation in *Arabidopsis*. *Plant J* **64**: 775–789
- Tusher VG, Tibshirani R, Chu G (2001) Significance analysis of microarrays applied to the ionizing radiation response. *Proc Natl Acad Sci USA* **98**: 5116–5121
- Ward JT, Lahner B, Yakubova E, Salt DE, Raghothama KG (2008) The effect of iron on the primary root elongation of *Arabidopsis* during phosphate deficiency. *Plant Physiol* **147**: 1181–1191
- Waters BM, McInturf SA, Stein RJ (2012) Rosette iron deficiency transcript and microRNA profiling reveals links between copper and iron homeostasis in *Arabidopsis thaliana*. *J Exp Bot* **63**: 5903–5918
- Wintz H, Fox T, Wu YY, Feng V, Chen W, Chang HS, Zhu T, Vulpe C (2003) Expression profiles of *Arabidopsis thaliana* in mineral deficiencies reveal novel transporters involved in metal homeostasis. *J Biol Chem* **278**: 47644–47653
- Yamasaki H, Abdel-Ghany SE, Cohu CM, Kobayashi Y, Shikanai T, Pilon M (2007) Regulation of copper homeostasis by micro-RNA in *Arabidopsis*. *J Biol Chem* **282**: 16369–16378
- Yamasaki H, Hayashi M, Fukazawa M, Kobayashi Y, Shikanai T (2009) SQUAMOSA Promoter Binding Protein-Like7 is a central regulator for copper homeostasis in *Arabidopsis*. *Plant Cell* **21**: 347–361
- Yang TJ, Lin WD, Schmidt W (2010) Transcriptional profiling of the *Arabidopsis* iron deficiency response reveals conserved transition metal homeostasis networks. *Plant Physiol* **152**: 2130–2141
- Yuan M, Li X, Xiao J, Wang S (2011) Molecular and functional analyses of COPT/Ctr-type copper transporter-like gene family in rice. *BMC Plant Biol* **11**: 69–81